

Quantitative analysis of surface plasmon interaction with silver nanoparticles

Andrey L. Stepanov

Institute of Physics and Erwin Schrödinger Institute for Nanoscale Research, Karl-Franzens-University Graz, Universitätsplatz 5, A-8010 Graz, Austria, and Kazan Physical-Technical Institute, Russian Academy of Sciences, Sibirsky Trakt 10/7, 420029 Kazan, Russian Federation

Joachim R. Krenn, Harald Dittlbacher, Andreas Hohenau, Aurelien Drezet, Bernhard Steinberger, Alfred Leitner, and Franz R. Aussenegg

Institute of Physics and Erwin Schrödinger Institute for Nanoscale Research, Karl-Franzens-University Graz, Universitätsplatz 5, A-8010 Graz, Austria

Received January 18, 2005

The present insight into plasmon effects on the nanoscale seems sufficiently advanced to allow the development of surface-plasmon-polariton- (SPP-) based optical devices. Therefore quantitative information describing SPP phenomena is required. We investigate a SPP beam splitter constituted by silver nanoparticles on a silver thin film, fabricated by electron-beam lithography. We acquire quantitative information on the beam splitter performance by monitoring SPP leakage radiation, yielding SPP reflection, transmission, and scattering efficiencies. © 2005 Optical Society of America

OCIS codes: 240.6680, 230.3990.

Owing to diffraction, the miniaturization of optical and optoelectronic devices is meeting a fundamental limitation to approximately half of the effective light wavelength. A potential solution to this problem is surface plasmon polaritons (SPPs), i.e., collective oscillations of conduction electrons at a metal-dielectric interface, coupled to a light field strongly localized at the interface.¹ SPP waves in an extended metal structure can be used for the propagation of light fields for signal transfer or optical addressing.^{2,3} The metals of choice are usually silver or gold because they show SPP modes in the visible or near-infrared spectral range in addition to having rather low ohmic damping.

Besides propagating SPPs, noble-metal nanoparticles have been known for a long time for spectrally selective absorption and scattering owing to localized particle plasmon excitation.⁴ Recent studies demonstrated that nanoparticle ensembles on metal thin films can act on SPPs and thus perform as optical elements in analogy with conventional optics such as mirrors or beam splitters.^{5,6} To image the spatial SPP profile, besides near-field optical microscopy,^{7,8} fluorescence imaging was applied. This technique relies on the fluorescence of organic molecules placed in the vicinity of the SPP-carrying metal surface.^{5,6,9} However, despite the advantages of fluorescence imaging for the visualization of SPP propagation, the practical application of this approach is restricted. First, fluorescence images have to be recorded within a limited time (typically a few seconds) after starting an experiment because of molecule bleaching. Second, the fluorescence intensity is in general not proportional to the local SPP field intensity,¹⁰ making quantitative measurements rather difficult. Therefore in the following we discuss and demonstrate another approach to imaging SPP fields by means of leakage radiation (LR).^{1,11,12} We demonstrate that this approach allows for quantitative measurements of the

spatial SPP field profile by deducing SPP reflection, transmission, and scattering efficiencies for a SPP beam splitter.

LR is emitted from the interface between a metal thin film and a higher-refractive-index medium (substrate), for example, glass. With respect to the interface normal, LR appears at a characteristic angle θ_{SPP} .¹ At this angle the LR wave in glass is phase matched to the SPP wave, satisfying $k_{\text{SPP}} = nk_0 \sin \theta_{\text{SPP}}$, where k_{SPP} and nk_0 are the wave vectors of the SPP and the LR, respectively, with n being the refractive index of glass. For glass with $n=1.5$ it follows that $\theta_{\text{SPP}} \approx 44^\circ$, which is larger than the critical angle of total internal reflection, $\theta_{\text{CRIT}} = 41.8^\circ$.^{11,12} Although LR contributes to SPP damping, it also permits the direct detection in the far field of the SPP spatial intensity distribution at the metal-air interface. Indeed, the spatial LR profile mirrors the SPP profile in both local intensity and azimuthal distribution.^{1,11,12} The experimental setup used for LR imaging is presented in Fig. 1. SPPs are excited locally by focusing polarized light from a Ti:sapphire laser at wavelengths λ_0 between 760 and 900 nm through a microscope objective (50 \times , numerical aperture of 0.7) onto the surface of lithographically nanostructured silver film (70 nm thick) on glass substrates (compare Fig. 2). Light-SPP coupling is mediated by a silver ridge (200 nm wide, 60 nm high) on the film surface.⁹ Just as the nanoparticle chains discussed in the following, the ridges are produced by first fabricating quartz ridges on the glass substrates by means of electron-beam lithography and electron-beam evaporation, which in a second step are covered with the silver thin film.

LR is detected by means of an oil-immersion objective (63 \times , numerical aperture of 1.25) and a CDD camera (see Fig. 1). Each pixel element of an image captures the flux of LR emerging from the corresponding position at the metal-air interface and is

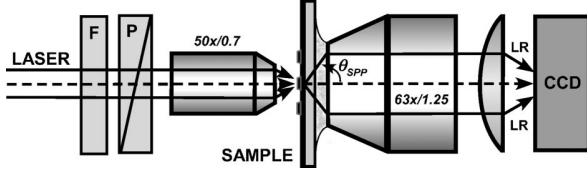


Fig. 1. Experimental scheme for LR imaging. SPPs are excited by focusing a laser beam onto a structured silver film on a glass substrate. LR is emitted into the glass substrate at an angle θ_{SPP} . F, gray filter; P, polarizer.

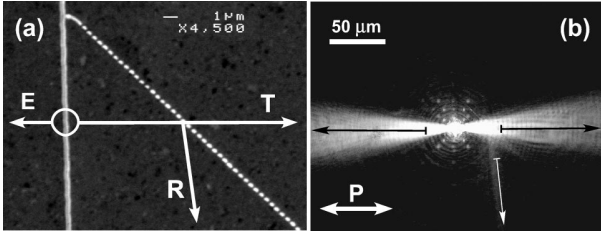


Fig. 2. SPP excitation and interaction with a nanoparticle beam splitter. (a) Scanning electron micrograph, showing the ridge for SPP launch and the nanoparticle chain constituting the beam splitter. The white circle marks the laser focus position; the arrows marked E, T, and R indicate the SPPs propagating freely to the left, being transmitted through the beam splitter, and being reflected, respectively. (b) Corresponding LR image for a laser wavelength of 800 nm. The arrows define the range of the cross cuts in Fig. 3; P indicates the polarization direction.

thus a direct quantitative measure of the SPP intensity at this position.

We now turn to the interaction of SPPs propagating on the 70 nm thick silver thin film with a beam splitter constituted by a chain of silver nanoparticles with a radius of 260 nm separated by a center-to-center distance of 400 nm. Figure 2(b) depicts the LR image ($\lambda_0=800$ nm) of such a sample, which is shown in the scanning electron micrograph in Fig. 2(a). We note that the center of the excitation at the position of the focused laser spot is overexposed in Fig. 2(b) because of the limited dynamic range of the CCD camera. As seen from Fig. 2(b), two highly directed SPP beams are excited, propagating to the right and left of the silver ridge.^{5,6} The SPP beam propagating to the right is incident on the nanoparticle chain under a mean angle of 45° with regard to the particle chain direction. The SPP is both partly reflected and transmitted by the beam splitter, as depicted by the arrows. The intensity of the reflected SPP beam is rather low for the present case of a single chain of nanoparticles compared with, e.g., multiple nanoparticle chains forming a Bragg mirror.⁵

Intensity cuts defined by the arrows in Fig. 2(b), corresponding to the directions E, T, and R as defined in Fig. 2(a), are shown in Fig. 3. The SPP intensity decay is evident together with spurious interference owing to the coherent character of the measurement. We fit these cuts by an expression describing the damped radiation from a dipole in two dimensions^{11,12},

$$I(x) = I_0 \frac{\exp[-(x+l)/t]}{x+l} + I_{\text{back}}, \quad (1)$$

where I is the determined SPP intensity, I_0 is the initial intensity of the SPPs, I_{back} is the value of the background intensity in the image, t is the decay constant of the SPPs, x is the distance from the focused laser spot, and l is the distance between the laser spot and the starting point for profile measurements in the images.

The quantitative analysis of the fit yields transmittance and reflectance values of 62% and 20%, respectively. Consequently, 18% remains to be attributed to scattering and absorption by the metal.

Next, we perform the quantitative analysis as a function of light wavelength, sweeping λ_0 from 760 to 900 nm. The resulting transmittance and reflectance data are summarized in Fig. 4. We find that in the near-infrared spectral region for wavelengths longer than ≈ 875 nm the beam splitter is almost transparent for the SPP ($T \approx 85\%$), whereas reflectance is very weak and cannot be measured; there-

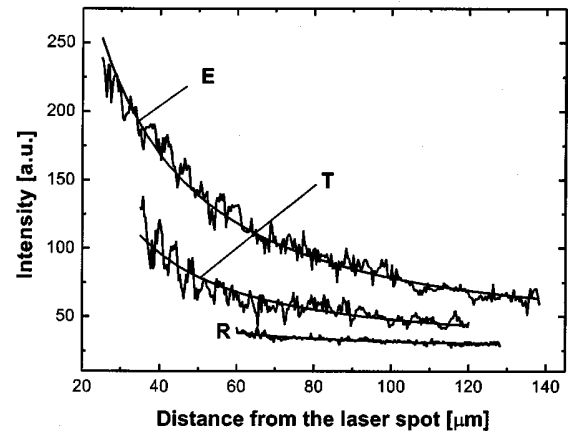


Fig. 3. Cuts of SPP intensity profiles along the arrows in Fig. 2(b), together with fits calculated by Eq. (1).

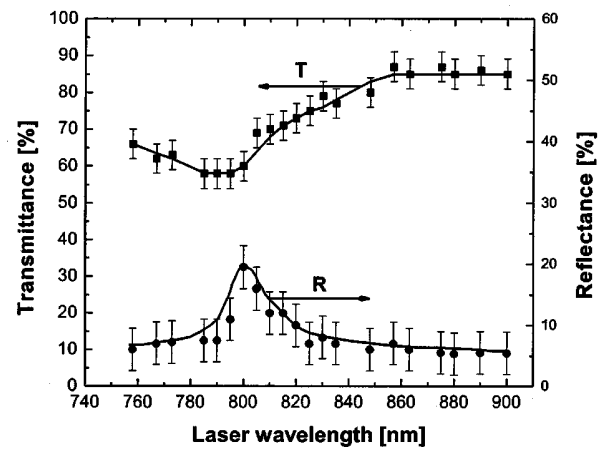


Fig. 4. Transmission (T) and reflection (R) efficiencies of the nanoparticle beam splitter in Fig. 2 versus laser light wavelength. Solid curve, guide to the eye.

fore $\approx 15\%$ of the incident SPP intensity has to be attributed to SPP scattering to light and absorption by metal. When moving toward shorter laser wavelengths, the transmittance monotonically decreases and has a minimum at ≈ 800 nm, whereas the reflectance simultaneously increases to a maximum value at the same wavelength. Proceeding further toward lower wavelengths restores the high transmittance and almost negligible reflectance values (Fig. 4). SPP transmittance and reflectance thus shows a resonancelike behavior with a resonance wavelength of approximately 800 nm. Although such resonances are well known from metal nanoparticles in dielectric matrices,⁴ our results show that nanoparticle-on-film systems maintain a resonant behavior in qualitative accordance with theoretical work.¹³

In summary, we have applied LR imaging for the quantitative experimental analysis of SPP interaction with a chain of silver nanoparticles. We found that SPP transmittance and reflectance show a resonance behavior, as expected from silver nanostructures. Quantitative data based on LR imaging might provide the basic input for the further development and optimization of subwavelength SPP-based optical devices.

For financial support the European Union under projects FP6 NMP4-CT-2003-505699 and FP6 2002-IST-1-507879 and the Lise Meitner program of the Austrian Scientific Foundation (M736-N08) are ac-

knowledge. A. L. Stepanov's e-mail address is andrey.stepanov@uni-graz.at.

References

1. H. Raether, *Surface Plasmons* (Springer, 1988).
2. J.-C. Weeber, Y. Lacroute, and A. Dereux, *Phys. Rev. B* **68**, 115401 (2003).
3. B. Lamprecht, J. R. Krenn, G. Schider, H. Ditlbacher, M. Salerno, N. Felidj, A. Leitner, F. A. Aussenegg, and J. C. Weeber, *Appl. Phys. Lett.* **79**, 51 (2001).
4. U. Kreibig and M. Vollmer, *Optical Properties of Metal Clusters* (Springer, 1995).
5. H. Ditlbacher, J. R. Krenn, G. Schider, A. Leitner, and F. R. Aussenegg, *Appl. Phys. Lett.* **81**, 1762 (2002).
6. J. R. Krenn, H. Ditlbacher, G. Schider, A. Hohenau, A. Leitner, and F. R. Aussenegg, *J. Microsc.* **209**, 167 (2003).
7. I. I. Smolyaninov, D. L. Mazzoni, J. Mait, and C. C. Davi, *Phys. Rev. B* **56**, 1601 (1997).
8. S. I. Bozhevolnyi, J. Erland, K. Leasson, P. M. W. Skovgaard, and J. M. Hvam, *Phys. Rev. Lett.* **86**, 3008 (2001).
9. H. Ditlbacher, J. R. Krenn, N. Felidj, B. Lamprecht, G. Schider, M. Salerno, A. Leitner, and F. R. Aussenegg, *Appl. Phys. Lett.* **80**, 404 (2002).
10. W. L. Barnes, *J. Mod. Opt.* **45**, 661 (1997).
11. A. Bouhelier, Th. Huser, H. Tamaru, H.-J. Güntherodt, D. W. Pohl, F. I. Baida, and D. Van Labeke, *Phys. Rev. B* **63**, 155404 (2001).
12. B. Hecht, H. Bielefeldt, L. Novotny, Y. Inouye, and D. W. Pohl, *Phys. Rev. Lett.* **77**, 1889 (1996).
13. R. Rupp, *Solid State Commun.* **39**, 903 (1981).